RARE METALS
Vol. 29, No. 1, Feb 2010, p. 37
DOI: 10.1007/s12598-010-0007-5

Corrosion behaviors of a new titanium alloy TZNT for surgical implant application in Ringer's solution

LI Jun[a], ZHOU Lian[b], and LI Zuochen[b]

[a] *School of Materials Engineering, Shanghai University of Engineering Science, Shanghai 201620, China*
[b] *Northwest Institute for Nonferrous Metal Research, Xi'an 710016, China*

Received 3 February 2009; received in revised form 18 March 2009; accepted 2 April 2009

Abstract

A new near α-titanium alloy Ti12.5Zr2.5Nb2.5Ta (TZNT) for surgical implants was designed. The potentiodynamic technique was performed to investigate the corrosion behaviors of TZNT in Ringer's solution, and Ti6Al4V, Ti6Al7Nb, and TA2 were taken as comparison. The structure of the passive film was analyzed using an X-ray photoelectron spectrometer (XPS). The results indicate that TZNT possesses better corrosion resistance, when compared with Ti6Al4V, Ti6Al7Nb, and TA2. The passive film formed on the TZNT surface is composed of oxides, such as TiO_2, ZrO_2, Nb_2O_5, and Ta_2O_5. The elements Zr and Ta are rich, whereas Ti and Nb are poor in the passive film. The addition of Zr, Nb, and Ta with relatively low electrochemical reaction potentials can reduce the anode activity and improve passive properties. Other than that, oxides such as ZrO_2, Nb_2O_5, and Ta_2O_5 with the nobler equilibrium constants make the passive film more stable.

Keywords: titanium alloy; surgical implant; electrochemistry; passive film; corrosion resistance

1. Introduction

Titanium alloys have been widely used for implant materials due to their excellent biocompatibility and corrosion resistance. Among these, Ti6Al4V as a kind of α + β titanium alloy is most frequently used as implant materials [1]. However, recent studies have shown that it possesses a high elastic modulus (about 120 GPa) which is gravely incompatible with that of human bones (about 28 GPa) [2]. Long-term experiments have confirmed that titanium implants with a high elastic modulus can transfer insufficient load to the adjacent remodeling bone and result in bone resorption and eventual loosening of prosthetic devices [3]. Moreover, reservations have been reported concerning the presence in long-term implants of the element vanadium which is toxic to the human body both in the elemental stat and as oxides [4-5]. Consequently, β-titanium alloys without toxic alloying elements and with a comparatively low elastic modulus are developed [6]. Unfortunately, the biomechanical compatibility of this kind of titanium alloys is not very satisfactory for admission strain (the ratio of yield strength and elastic modulus) of about 1% is higher than that of human bones (about 0.67%), which is another important parameter to characterize the biomechanical compatibility of titanium alloys besides the elastic modulus [7]. The shortcoming for β-titanium alloys is inevitable owing to their high yield strength and relatively low elastic modulus.

Based on the above analysis and the clinical requirements for surgical implants, a new near-α titanium alloy with a low aluminum equivalent content for restorative and prosthodontic materials was designed by the d-electron alloy design theory. Toxicity-free elements such as Zr, Nb, and Ta are selected as intensification elements, which have been extensively evaluated and identified as producing no adverse tissue reactions [8]. Considering the effects of three kinds of alloying elements on strength of the titanium alloy, the contents for Zr, Nb, and Ta were ascertained. The new titanium alloy was named as Ti12.5Zr2.5Nb2.5Ta (TZNT) which has been certified to possess approximately equivalent admission strain (0.65%) with that of human bones (0.67%); other than that, the elastic modulus is lower (about 100 GPa) than that of Ti6Al4V (about 120 GPa) [9].

As a new titanium alloy for biomedical applications, evaluation of the corrosion behaviors is very crucial for corrosion properties have close relation with other properties such as biocompatibility and mechanical properties, which can cause a release of those alloying elements to the surrounding tissue [10]. Extensive release of ions from prosthe-

Corresponding author: LI Jun **E-mail:** jacob_lijun@sina.com

sis can result in adverse biological reactions and lead to mechanical failure of the device. Therefore, various in vitro and in vivo tests have to be carried out to identify appropriate materials for use as surgical implants. It is desirable to keep metal ions release to a minimum by the use of corrosion-resistant materials, to a large extent, which depends on the stable passive film formed on the surface to provide a barrier between the bio-environment and the alloy substrate [11].

Obviously, no detailed information with respect to the corrosion behaviors of the new titanium alloy in Ringer's solution could be found in the literatures. The objective of this research was to study the corrosion behaviors of TZNT in the simulated physiological fluid by the potentiodynamic polarization technique in comparison with that of TA2, Ti6Al4V, and Ti6Al7Nb. Accompanied with the analysis about the structure of the passive film formed on the surface of TZNT by means of an X-ray photoelectron spectrometer (XPS), the corrosion mechanism was analyzed in detail.

2. Experimental

Ingots of 10 kg with a nominal composition of Ti12.5Zr2.5Nb2.5Ta (TZNT) were manufactured by homogeneously melting the special intermediate alloys in a conventional consumable electrode vacuum arc melting furnace. Each ingot was twice melted to ensure homogeneity, and the chemical analysis results are given in Table 1. The testing composition is approximately equivalent with the nominal composition. A portion of the alloy was forged into 16 mm diameter rolled bar and machined into testing specimens of 16 mm in diameter and 1.5 mm in thickness. Then they were polished on a Buehler Phoenix 4000 sample preparation system and rinsed with alcohol and acetone. Commercial Ti6Al4V, Ti6Al7Nb, and TA2 as reference materials were obtained in the form of rods and were dealt with according to the above procedure.

Table 1. Chemical composition of TZNT wt.%

Chemical composition	Ti	Zr	Nb	Ta
Nominal composition	82.5	12.5	2.5	2.5
Testing composition	82.3	12.4	2.5	2.8

The corrosion behaviors for four types of materials were tested and evaluated by means of the potentiodynamic polarization technique in 1000 mL Ringer's solution of pH 7.4 (the chemical composition is shown in Table 2) at 37°C which is equivalent to human body temperature. Prior to the polarization tests, the specimens were immersed in Ringer's solutions for 2 h to reach a steady state with stable open circuit potential. The tests were carried out by means of a model 351 EG&G PARC electrochemical test system. A standard three-electrode cell composed of the investigated titanium alloys as the working electrodes with 1 cm^2 exposed area, a saturated calomel reference electrode (SCE), and a graphite counter electrode were used to perform the polarization experiments. Scanning rate in dynamic potential was 1 mV/s, and the potential was varied from –0.25 to 3.75 V.

Table 2. Chemical constitution of Ringer's solution

NaCl / g	$NaHCO_3$ / g	$CaCl_2 \cdot 6H_2O$ / g	KCl / g	Distilled water / mL
9.00	0.20	0.25	0.40	1000

The structure of the passive film formed on the TZNT surface after applying a potential of 1 V located in the first passive region for 20 min was studied by means of a VG ESCALABMK II X-ray photoelectron spectrometer (XPS). XPS spectra were acquired in the Fixed Analyzer Transmission (FAT) mode and corrected by the C1s peak with 284.6 eV bonding energy, using an Mg K_α (12.54 eV) as the excitation source. Argon-ion-sputter was applied at 4 keV for 5 min to eliminate contaminant. The vacuum level of the analyzing chamber during measurement was of the order of 1×10^{-5} Pa. Chemical composition was calculated by the relative atomic sensitivity factors [12]:

$$C_x = \frac{\rho_x}{\sum_i \rho_i} = \frac{I_x / S_x}{\sum_i I_i / S_i} \quad (1)$$

where C_x is the atomic concentration of the element x, ρ is the atomic density, I is the intensity for the corresponding peak, and S is the relative atomic sensitivity factor.

3. Results and discussion

The isolated corrosion potential is a stable potential in a corrosion system without polarization, which demonstrates the thermodynamic characteristics of the objects and the surface state of the electrode. Contact corrosion is often observed in human bodies due to existence of more than two kinds of metals. Based on the electrochemical principles, the more negative the isolated corrosion potential is, the more remarkable the corrosion inclination is. Thus, two kinds of contact materials can be divided into an anode and a cathode, one metal as the anode with a lower isolated corrosion potential will be seriously dissolved, and the other will be protected from corrosion. The isolated corrosion potentials for four tested materials were obtained as shown in Table 3. The isolated corrosion potentials for TZNT, Ti6Al7Nb, Ti6Al4V, and TA2 are –0.204, –0.245, –0.306, and –0.347 V; the

corrosion trend of these materials is as follows: TA2 > Ti6Al4V > Ti6Al7Nb > TZNT, which indicates that TZNT is the most stable in comparison with other materials in Ringer's solution.

Table 3. Results of electrochemical corrosion tests for four materials

Material	E_{corr} / V	E_f^1 / V	E_t / V	E_0 / V	E_f^2 / V	I_p^1 / (μA·cm^{-2})	I_0 / (μA·cm^{-2})	I_p^2 / (μA·cm^{-2})
TZNT	–0.204	0.11	1.43	1.78	1.93	7.58	15.85	18.63
Ti6Al7Nb	–0.245	0.12	1.32	1.80	2.14	7.09	173.78	77.62
Ti6Al4V	–0.306	0.23	1.24	2.22	2.70	10.00	15848.93	1378.96
TA2	–0.347	0.39	1.36	1.90	2.33	28.18	1412.54	147.91

Note: E_{corr} is the isolated corrosion potential, E_f^1 and E_t are the low limit and high limit potentials in the first passive region, respectively, I_p^1 is the current density in the first passive region, E_0 is the potential in correspondence with the highest current density, I_0 is the highest current density during the whole scanning range, E_f^2 is the low limit potential in the re-passive region, and I_p^2 is the current density in the re-passive region.

Fig. 1 shows the potentiodynamic polarization curves of TZNT, Ti6Al7Nb, Ti6Al4V, and TA2 in Ringer's solution at a pH of 7.4 and a temperature of 37°C. The related corrosion parameters obtained from the potentiodynamic polarization scans are displayed in Table 3. As shown in Fig. 1, the polarization curves of the Ti-based alloys and TA2 are divided into five regions. For the first region, the alloying elements are oxidized into ions with different valences and the formation of the passive films is carried on in parallel with the reactions, which demonstrates that the electrodes are in the active-passive state. Because the reactions are predominant over the formation of the passive films, the current density increases with the increase in potential. When the potential approaches E_f^1, the electrodes transfer from the active-passive state to the passive state, the current densities remain very stable with the increase in potential in this region, about 7.58, 7.09, 10.00, and 28.18 μA·cm^{-2} for TZNT, Ti6Al7Nb, Ti6Al4V, and TA2, indicating that the passive films were steadily formed on the electrode surface. With the increase in potential, the abrupt increase in current density is observed for three materials Ti6Al7Nb, Ti6Al4V, and TA2 except TZNT at different potentials, about 1.32, 1.24, and 1.36 V, which should be attributed to the destruction of the passive films by chlorine ions from the solution. Some fields of the electrodes, which were protected by passive films from corrosion once, are exposed to the solution once again and the alloying elements such as Ti, Zr, and Al take part in the charge transfer with the increase in potential. When the potentials rise to about 1.78, 1.80, 2.22, and 1.90 V for TZNT, Ti6Al7Nb, Ti6Al4V, and TA2, respectively, the corresponding current densities also reach the maximum values, about 15.85, 173.78, 15848.93, and 1412.54 μA·cm^{-2}. Along with further increase in potential, the restoration of the breakdown portions on the passive films is carried on and gradually becomes dominant over the reactions. Finally, the current densities are fixed on the relatively stable values of about 18.63, 77.62, 1378.96, and 147.91 μA·cm^{-2} for four materials, TZNT, Ti6Al7Nb, Ti6Al4V, and TA2, indicating that the electrodes formally enter into the re-passive state.

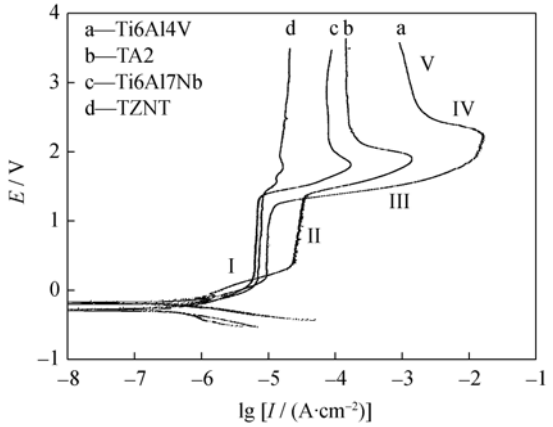

Fig. 1. Polarization curves of four materials.

The passive behaviors can be used to assess the passivity inclination of the materials and the relative stabilization of the passive films in the given environment by the potentiodynamic polarization technique. Three parameters such as E_f^1 for the first passive region, E_0 and I_0 for the re-passive region are related to the former. E_f^1 characterizes the difficulty into the first passive state. The closer it is to the isolated corrosion potential, the easier the system is to be passive, and the materials are earlier protected from corrosion. When I_0 is low, the areas subjected to spot corrosion are small and the restoration time for the passive films is correspondingly short. As a result, the electrodes are easier to change from the active state to the re-passive state. Similarly, it is beneficial for the system to step into the re-passive stage when E_0 in correspondence with I_0 is small. As shown in Fig. 1 and Table 3, among four materials, TZNT possesses the smallest values for E_f^1, E_0, and I_0. Grounded on the above analysis, it can be concluded that TZNT enters the passive state more easily.

The stability of the passive films is characterized by two parameters: the potential range and the passive current density in the passive state. The broader the potential range is, the more difficult it is for the passive films to transform from the passive state into the active state. On the other hand, the passive current densities are small whether in the first passive or in the re-passive state, and the dissolution speed of the passive films is relatively low, indicating that the passive films are more stable. For TZNT, Ti6Al7Nb, Ti6Al4V, and TA2, the potential ranges in the first passive region are 1.32, 1.20, 1.01, and 0.97 V. Obviously, TZNT has the broadest potential range. Similarly, the passive current densities for TZNT are low whether in the first passive region or in the re-passive region; they are 7.58 and 18.63 $\mu A \cdot cm^{-2}$, respectively. The above analysis shows that the passive film formed on the TZNT surface is the most stable in comparison with the remains.

Among four materials, the passive properties of three kinds of Ti-based alloys are better than that of TA2 due to the addition of the alloying elements such as V, Al, Zr, Nb, and Ta which contribute to reducing the anode activity and promoting passivity. To further investigate the corrosion mechanism of TZNT which outmatches two kinds of Ti-based alloys, the composition and quantivalence of each element for the passive film were analyzed by XPS. Fig. 2 shows the XPS survey spectrum over the wide binding energy region for the passive film of TZNT. The spectrum mainly consists of electron peaks Ti2p, Zr3d, Nb3d, Ta4f, and O1s throughout the whole scanning, which indicates that the passive film is mainly composed of Ti, Zr, Nb, Ta, and O elements.

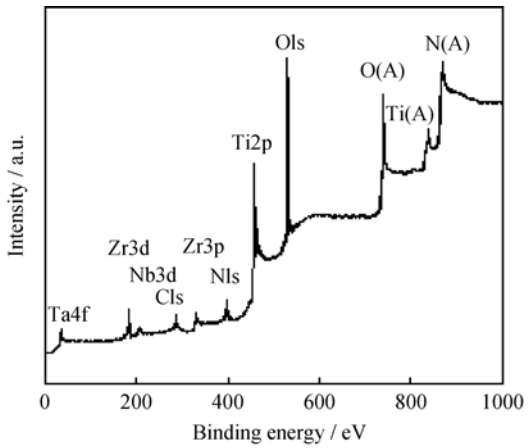

Fig. 2. XPS survey spectrum for the passive film of the TZNT surface.

Figs. 3(a)-3(e) show the typical Ti2p, Zr3d, Nb3d, Ta4f, and O1s XPS spectra. Combining with the comparison between experimental data and standard data of binding energy as presented in Table 4, the structure of the passive film can be further confirmed. The Ti2p XPS spectrum is composed of $2p_{3/2}$ (458.4 eV) and $2p_{1/2}$ (463.7 eV) electron peaks that represent the existence of TiO_2. The Zr3d XPS spectrum includes $3d_{5/2}$ (181.7 eV) and $3d_{3/2}$ (184.1 eV) electron peaks revealing the presence of ZrO_2. The Nb3d XPS spectrum only consists of a very broad electron peak which may result from the overlapping of two electron peaks with approximately equivalent binding energy: the one is $Nb3d_{5/2}$ with binding energy 207.4 eV, and the other is $Nb3d_{3/2}$ with binding energy 207.2 eV. As shown in Table 4, the analysis result of the Nb3d XPS spectrum reveals the presence of Nb_2O_5. In the case of the Ta4f XPS spectrum, two peaks are also found, associated with the metallic form (substrate) and the oxide form, Ta_2O_5, present in the passive film. The second electron peak is broader, which can be discomposed into two peaks with about the same binding energy: one is $Ta4f_{7/2}$ with a binding energy of 26.6 eV, and the other is $Ta4f_{5/2}$ with a binding energy of 26.7 eV. The O1s XPS spectrum shown in Fig. 3(e) only includes a very strong peak indicating the presence of metal oxides for elements Ti, Zr, Nb, and Ta (as shown in Table 4), which further substantiates the above analysis. Based on the analysis results, it is concluded that the passive film on the TZNT surface consists of four metallic oxides which are TiO_2, ZrO_2, Nb_2O_5, and Ta_2O_5. Similar results were obtained in Ref. [13].

Moreover, quantitative analysis of XPS data indicates that the chemical composition (at.%) in terms of four metal elements is Ti : Zr : Nb : Ta = 71.61 : 9.56 : 1.24 : 17.59 in the oxide film, which is significantly different from that of the bulk (Ti : Zr : Nb : Ta = 90.64 : 7.21 : 1.42 : 0.73 (at.%)). The Ti concentration is decreased from 90.64% in the bulk to 71.61% in the passive film. With respect to the Nb concentration, the change is not obvious, and there is only a little decrease. On the contrary, the concentration for the other two elements Zr and Ta is improved; particularly for Ta, the concentration is abruptly increased about twenty three times. The difference can be described by the enrichment factor [14].

$$f(\mathrm{Me}) = \frac{\mathrm{Me/TZNT\ (in\ the\ passive\ film)}}{\mathrm{Me/TZNT\ (in\ the\ body)}} \quad (2)$$

where Me/TZNT (in the passive film) is the atomic percent for the element Me which represents Ti, Zr, Nb, and Ta in the passive film; and Me/TZNT (in the body) is the atomic percent for some elements in the bulk.

According to the calculation, the enrichment factors for Ti, Zr, Nb, and Ta are 0.79, 1.32, 0.87, and 24.10. f(Ti) and f(Nb) are less than 1, whereas f(Zr) and f(Ta) are beyond 1, which indicates the elements Ti and Nb are poor and Zr and Ta are rich in the passive film.

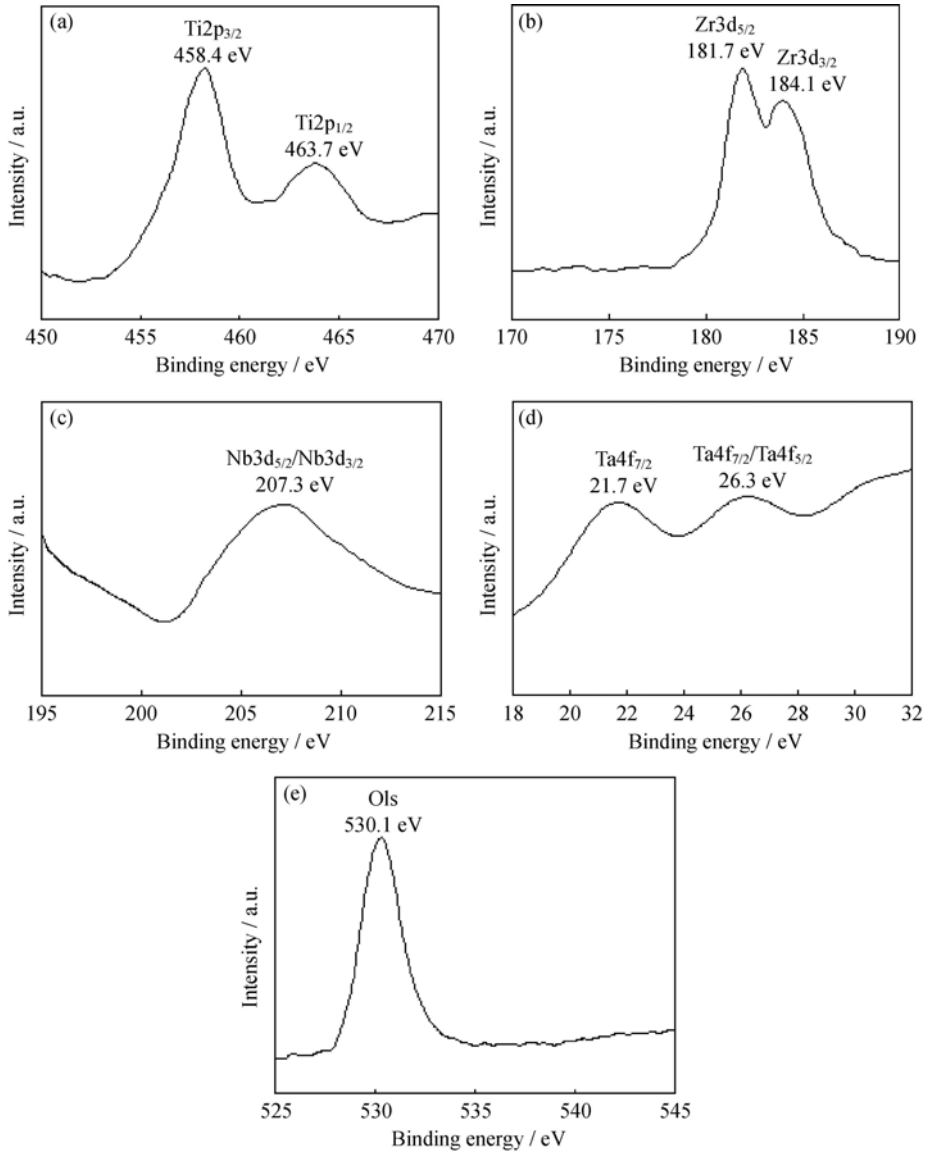

Fig. 3. XPS spectra for the passive film of the TZNT surface: (a) Ti2p region, (b) Zr3d region, (c) Nb3d region, (d) Ta4f region, and (e) O1s region.

Table 4. Comparison between experimental data and standard data of binding energy

Element	Experimental data of binding energy / eV	Standard data of binding energy / eV	Standard element	Chemical bonding
Ti	458.4	458.5	$Ti2p_{3/2}$	TiO_2
	463.7	463.6	$Ti2p_{1/2}$	TiO_2
Zr	181.7	182.0	$Zr3d_{5/2}$	ZrO_2
	184.1	185.3	$Zr3d_{3/2}$	ZrO_2
Nb	207.3	207.4	$Nb3d_{5/2}$	Nb_2O_5
	207.3	207.2	$Nb3d_{3/2}$	Nb_2O_5
Ta	21.7	21.5	$Ta4f_{7/2}$	Ta
	26.3	26.6	$Ta4f_{7/2}$	Ta_2O_5
	26.3	26.7	$Ta4f_{5/2}$	Ta_2O_5
O	530.1	530.1	O1s	TiO_2
		530.0	O1s	ZrO_2
		530.4	O1s	Nb_2O_5
		530.4	O1s	Ta_2O_5

The difference may be attributed to the difference in electrode reactions occurring at different potentials and oxide stabilities. The following electrochemical reactions can take place based on Ref. [15-16].

$$\text{For Ti element}\begin{cases}\text{Ti(II)} \rightleftharpoons \text{Ti(0)} & \text{Ti}^{2+}+2\text{e} \rightleftharpoons \text{Ti} \quad \varphi = -1.630\ \text{V} \quad (3)\\ \text{Ti(III)} \rightleftharpoons \text{Ti(II)} & \text{Ti}^{3+}+\text{e} \rightleftharpoons \text{Ti}^{2+} \quad \varphi = -0.900\ \text{V} \quad (4)\\ \text{Ti(VI)} \rightleftharpoons \text{Ti(0)} & \text{TiO}_2+4\text{H}^{+}+4\text{e} \rightleftharpoons \text{Ti}+2\text{H}_2\text{O} \quad \varphi = -0.860\ \text{V} \quad (5)\end{cases}$$

$$\text{For Zr element}\quad \text{Zr(IV)} \rightleftharpoons \text{Zr(0)} \qquad \text{ZrO}_2+4\text{H}^{+}+4\text{e} \rightleftharpoons \text{Zr}+2\text{H}_2\text{O} \quad \varphi = -1.553\ \text{V} \quad (6)$$

$$\text{For Nb element}\begin{cases}\text{Nb(III)} \rightleftharpoons \text{Nb(0)} & \text{Nb}^{3+}+3\text{e} \rightleftharpoons \text{Nb} \quad \varphi = -1.099\ \text{V} \quad (7)\\ \text{Nb(V)} \rightleftharpoons \text{Nb(0)} & \text{Nb}_2\text{O}_5+10\text{H}^{+}+10\text{e} \rightleftharpoons 2\text{Nb}+5\text{H}_2\text{O} \quad \varphi = -0.644\ \text{V} \quad (8)\end{cases}$$

$$\text{For Ta element}\quad \text{Ta(V)} \rightleftharpoons \text{Ta(0)} \qquad \text{Ta}_2\text{O}_5+10\text{H}^{+}+10\text{e} \rightleftharpoons 2\text{Ta}+5\text{H}_2\text{O} \quad \varphi = -0.750\ \text{V} \quad (9)$$

According to the standard chemical potentials against standard hydrogen electrode at 25°C, these electrochemical reactions follow the order: (3) > (6) > (7) > (4) > (5) > (9) > (8). Combined with analyses results of potentiodynamic polarization and XPS, the growth behavior of the passive film can be represented by physical illustration shown in Fig. 4, where the growth process of the passive film is divided into six steps.

(1) Prior the electrochemistry test, the specimen exposed to the air is subjected to forming metal oxides (thickness 1 to 4 nm) on the alloy surface, which is not very compact, considering that titanium and other alloy elements present

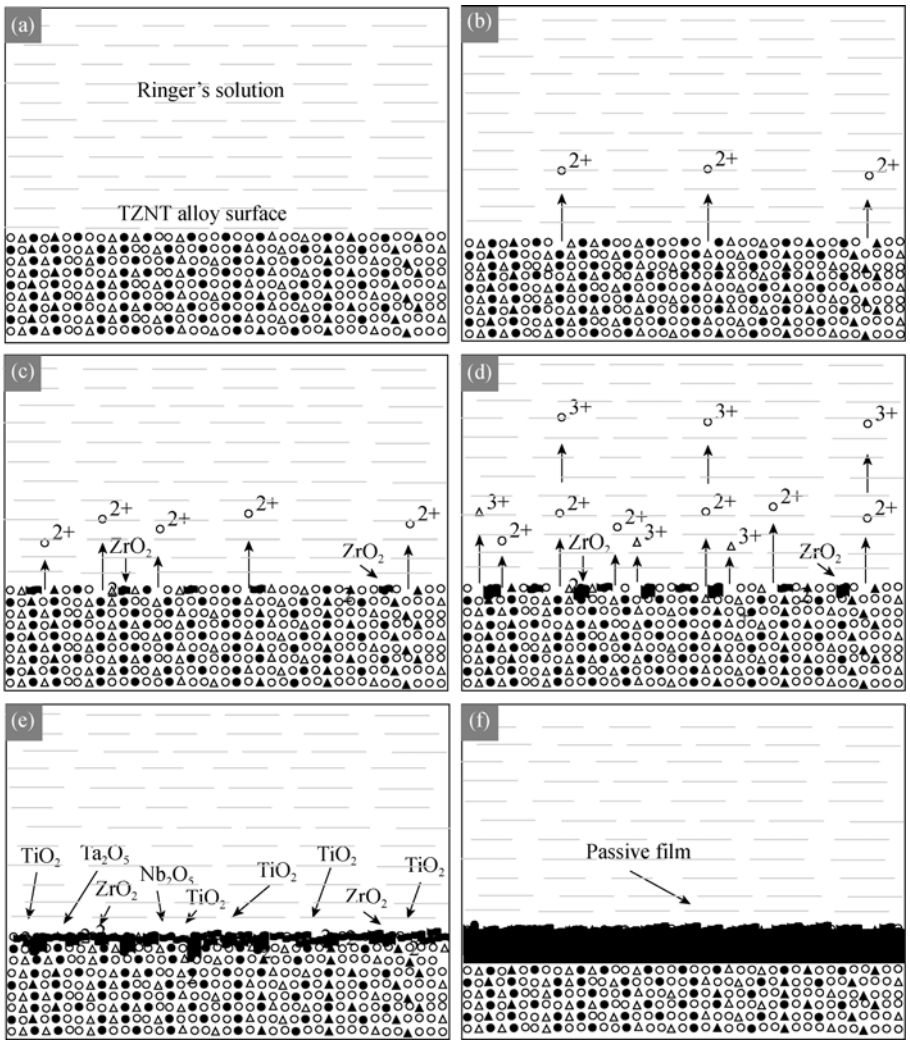

Fig. 4. Physical illustration for the growth behaviors of the passive film: ○ Ti atoms; ● Zr atoms; Δ Nb atoms; ▲ Ta atoms.

greater affinity to the oxygen [17].

(2) As presented in Fig. 4(b), with the rapid increase in potential from the initial scanning value, the element Ti can be dissolved into the solution with two valence electrons, resulting in the poorness of Ti in the passive film.

(3) During this process, the element Zr is firstly turned into ZrO_2, as analyzed by XPS, unlike the element Ti which enters into the solution with the ion form. It indicates that ZrO_2 along with other oxides spontaneously formed on the surface establish the barrier and inhibit the dissolution of metal elements to a certain extent. The Zr concentration has little loss in the passive film as demonstrated in the quantitative analysis of XPS.

(4) Following the formation of ZrO_2, the element Nb is also transformed into Nb^{3+} and takes part in the charge transfer with the further increase in potential. It leads to low concentration in the passive film compared with the bulk, which is in accordance with the XPS results. At the same time, the parallel reactions (3) and (6) proceed.

(5) When the potential further increases to some value, the elements Ti, Ta, and Nb are turned into three kinds of oxides according to the reactions (5), (8), and (9) for they possess the approximately equivalent standard chemical potentials. As a result, a thick, adherent, and uniform passive film is formed on the TZNT surface, and the electrode is transformed from the active-passive state into the passive state as shown in Fig. 1. Similar to the element Zr, the element Ta is directly changed into the oxide form from the elementary form and the concentration is relatively improved due to the loss of the elements Ti and Nb.

(6) At this step corresponding with the first passive region, thickness of the passive film gradually increases with the increase in potential as shown in Fig. 4(f). Other than that, the latent hazard for spot corrosion occurring on the passive film gradually progresses, which can destroy the integrity of the passive film and make the corrosion system correspondingly come into the active zone, i.e. the third region owing to the irregular absorption of chlorine ions and the formation of freely soluble complex ions on the passive film's surface, particularly at some spots with defects. Consequently, spot nuclei are formed and the current density correspondingly increases.

Difference of the passivity inclination of four materials and relative stabilization of the passive films in the given environment can be explained by the above physical model. For Ti6Al4V and TA2, passivity is mainly attributed to the formation of TiO_2; however, for TZNT and Ti6Al7Nb, besides the formation of TiO_2, the alloying elements Zr, Nb, and Ta added into pure titanium can also be quickly transformed into the oxides in a relative low potential, which form a barrier along with TiO_2. For this reason, TZNT and Ti6Al7Nb can earlier enter into the passive state as presented in Fig. 1. Relatively speaking, the initial potential into the passive region for TZNT is lower due to the prior formation of ZrO_2 in comparison with other oxides. Compared with other materials, TZNT also possesses the relatively stable and lower current density and a broader passive potential range in the passive state, showing that the passive film formed on the TZNT surface is more stable and is more difficult to break. The stabilization of the passive films is closely related to that of the oxides. The physicochemical properties of some pure metals and their oxides are shown in Table 5. Ta_2O_5 and Nb_2O_5 possess more positive equilibrium constants, indicating that the passive film consisting of these compounds is more stable and is difficult to dissolve into the solution, so TZNT possesses the broadest potential range and the lowest current density in the first passive region. Based on the above analysis, it is very easy to explain the subsequent processes, that is why the alloy TZNT can enter into the second region from the active and active-passive states more quickly and has the lowest current density in comparison with the other materials.

Table 5. Physicochemical properties of some pure metals and their oxides [16, 18-19]

Element	Oxide	Relative dielectric constant, ε	Formation enthalpy, ΔH_{298} / (kJ·mol^{-1})	Solubility, pK	Biocompatibility
V	V_2O_5	Not available	–1558	10	Toxic
Al	Al_2O_3	5-10	–1680	15	Potentially necrotic
Ti	TiO_2	110	–945	18	Inertness
Zr	ZrO_2	10-18	–1088	17	Inertness
Nb	Nb_2O_5	280	–794	20	Inertness
Ta	Ta_2O_5	12	–2054	20	Inertness

4. Conclusions

(1) The newly developed titanium alloy TZNT for surgical implants possesses a better corrosion resistance in Ringer's solution, from two points of view, the passivity inclination of the materials and the relative stabilization of the passive film, in comparison with Ti6Al7Nb, Ti6Al4V, and TA2.

(2) The passive film formed on the TZNT surface is composed of the oxides, such as TiO_2, ZrO_2, Nb_2O_5, and Ta_2O_5, based on the results of XPS. The elements Zr and Ta are rich, but the elements Ti and Nb are poor in passive films.

(3) The addition of the elements Zr, Nb, Ta, V, and Al into pure Ti can reduce the anode activity and further improve passive properties. Comparatively, ZrO_2, Nb_2O_5, and Ta_2O_5 possess the nobler equilibrium constants; that is why TZNT with Zr, Nb, and Ta as alloying elements has a better corrosion resistance.

Acknowledgement

This work was financially supported by the Shanghai Science and Technology Development Foundation, China (No. 08QA14035).

References

[1] Karayan A.I., Park S.W., and Lee K.M., Corrosion behavior of Ti-Ta-Nb alloys in simulated physiological media, *Mater. Lett.*, 2008, **62**: 1843.

[2] Geetha M., Singh A.K., Muraleedharan K., Gogia A.K., and Asokamani R., Effect of thermomechanical processing on microstructure of a Ti-13Nb-13Zr alloy, *J. Alloys Compd.*, 2001, **329**: 264.

[3] Geetha M., Kamachi Mudali U., Gogia A.K., Asokamani R., and Raj B., Influence of microstructure and alloying elements on corrosion behavior of Ti-13Nb-13Zr alloy, *Corros. Sci.*, 2004, **46**: 877.

[4] Khan M.A., Williams R.L., and Williams D.F., The corrosion behaviour of Ti-6Al-4V, Ti6Al-7Nb and in protein solutions, *Biomaterials*, 1999, **20**: 631.

[5] Wapner K.L., Implications of metallic corrosion in total knee arthroplasty, *Clin. Orthop. Relat. Res.*, 1991, **271**: 12.

[6] Nilson T.C., Aleixo G., Caramb R., and Guastaldi A.C., Development of Ti-Mo alloys for biomedical applications: Microstructure and electrochemical characterization, *Mater. Sci. Eng. A*, 2007, **452-453**: 727.

[7] Steinemann S.G., Mausli P.A., and Semlitach M., Titanium science and technology, [in] *Titanium'92 Science and Technology*, 1993: 2689.

[8] Li S.J., Yanga R., Lia S., Hao Y.L., Cui Y.Y., Niinomi M., and Guo Z.X., Wear characteristics of Ti-Nb-Ta-Zr and Ti-6Al-4V alloys for biomedical applications, *Wear*, 2004, **257**: 869.

[9] Li J., Zhou L., Li Z.C., and Chen D.J., Study of a new titanium alloy for surgical implant application, *Rare Met. Mater. Eng.* (in Chinese), 2003, **32**(5): 398.

[10] Eisenbarth E., Velten D., Uller M.M., Thull R., and Breme J., Biocompatibility of β-stabilizing elements of titanium alloys, *Biomaterials*, 2004, **25**: 5705.

[11] Gurappa I., Characterization of different materials for corrosion resistance under simulated body fluid conditions, *Mater. Charact.*, 2002, **49**:73.

[12] Li G.W., Wu Z.L., Shao S.Z., and Liu Z.K., XPS studies on ZnO/Si grown by O^+-assisted PLD, *Mater. Sci. Technol.*, 2008, **16**(2): 254.

[13] Pang S.J., Shek C.H., Zhang T., Asami K., and Inoue A., Corrosion behavior of glassy $Ni_{55}Co_5Nb_{20}Ti_{10}Zr_{10}$ alloy in 1 N HCl solution studied by potentiostatic polarization and XPS, *Corros. Sci.*, 2006, **48**: 625.

[14] Castle J.E. and Qiu H.A., Coordinated study of the passivation of alloy steel by plasma source mass spectrometry and X-ray photoelectron spectroscopy-I, *Corros. Sci.*, 1989, **29**(5): 591.

[15] Wang X.Y. and Ma F.X., *Inorganic and Analytical Chemistry*, Chemistry Industry Press, Beijing, 2009:289.

[16] Liang Y.J., *Physical Chemistry*, Metallurgy Industry Press, Beijing, 1995:310.

[17] Masmoudi M., Capek D., Abdelhedi R., Halouani F.E., and Wery M., Application of surface response analysis to the optimisation of nitric passivation of cp titanium and Ti6Al4V, *Surf. Coat. Technol.*, 2006, **200**: 6651.

[18] Steinemann S.G. and Perren S.M., Titanium science and technology, [in] *Proceedings of the Fifth International Conference on Titanium*, Munich, 1984: 1327.

[19] Jonsson A.K., Niklasson G.A., and Veszelei M., Electrical properties of ZrO_2 thin films, *Thin Solid Films*, 2002, **402**: 242.